ELSEVIER

Catalysis Today 47 (1999) 325–338

CATALYSIS TODAY

Application concepts and evaluation of small-scale catalytic combustors for natural gas

Hiroki Sadamori

Fundamental Research Laboratories, Osaka Gas Co., Ltd., 6-19-9 Torishima, Konona-ku, Osaka 554, Japan

Abstract

Basic application concepts of catalytic combustion are roughly classified into three types, and the development of catalysts, combustion performance and applicability are stated. On the diffusive catalytic combustion method, completeness of methane combustion and its reaction mechanism have been demonstrated by detailed combustion analysis of the burner and reaction kinetics. On the adiabatic lean premixed catalytic combustion method, applicability of a high-temperature catalyst system based on Mn-substituted hexaaluminate monolithic honeycomb to a 1.5 MW gas turbine combustor has been investigated through pressurized combustion tests and prototype engine-rig tests. As a result, a good outlook of the basic technical problems to overcome including the catalyst durability and the combustor control method was obtained, but another problem was that of the combustor capacity. In view of the progress of the non-catalytic lean premixed combustion method, it was concluded that a hybrid catalytic combustion method limiting catalytic combustion to the low-temperature range in this concept might become efficient in the future, but that it would depend on the development of efficient catalysts initiating their activity at about 350°C and having durability at 1000°C.

Keywords: Catalytic combustion; Mn-substituted hexaaluminate; Diffusive catalytic combustion; Premixed catalytic combustion; Hybrid catalytic combustion

1. Introduction

Reduction of NO_x emissions and increase of safety and efficiency in the natural gas combustion process have recently become even more important since the demand of natural gas as an energy source has been increasing worldwide.

Catalytic combustion of natural gas has been attracting attention since the mid-1970s when natural gas came to be used worldwide, and various kinds of application concepts have been proposed.

The concepts are roughly classified into the following three types:

1. *Diffusive catalytic combustion method*. In this concept, a fiber-mat catalyst is used. Fuel supplied from the back side without premix-air is burnt by almost catalytic oxidation with oxygen diffusing from the front side, radiating energy from the surface at temperatures less than 600°C. It has potentialities of wide use not only in residential, but also in industrial areas because of its high far-infrared radiation efficiency and nearly absent NO_x emissions.
2. *Adiabatic lean premixed catalytic combustion method*. In this concept, a honeycomb-shaped catalyst is used. A preheated lean fuel–air mixture whose adiabatic temperature is less than 1500°C is introduced into the catalyst system and is burnt under almost adiabatic conditions by both catalytic and gas-phase oxidation. This concept has been

0920-5861/99/$ – see front matter
PII: S0920-5861(98)00314-9

attracting attention as a very low-NO_x combustor concept for gas turbines. Initially, it was thought that high-temperature-durable catalysts were inevitable to realize such combustors, but now studies of a hybrid catalytic combustion system consisting of a low-temperature catalytic combustion zone and a gas-phase combustion zone behind the catalyst are actively carried out.

3. *Radiant premixed catalytic combustion method*. In this concept, catalysts of various shapes, e.g. honeycomb, cloth, tube, and particles are used. A premixture of fuel and air introduced into the catalyst is burnt by both catalytic and gas-phase oxidation, radiating energy from the catalyst surface. Its application to residential and industrial areas has been investigated, expecting lower NO_x emissions and higher radiation efficiency than those of conventional homogeneous combustion methods.

Commercialization of these concepts fueled by natural gas greatly depends on the development of efficient catalysts with high activity, high durability, and low cost. However, it is not very easy to develop such catalysts, because the catalytic reactivity of natural gas is intrinsically lower than that of petroleum gas.

This paper summarizes application concepts and evaluation of small-scale natural gas catalytic combustors less than 1.5 MW which the author has been investigating.

2. Diffusive catalytic combustion method

Fig. 1 shows the basic construction of the diffusive catalytic combustion method. It may have been developed in 1916 in France as an engine warmer for airplanes. Currently, portable heaters fueled by LPG are prevailing worldwide. Catalytic combustion in the heater quickly starts by instant surface combustion with a flame with nearly no fuel slippage. The combustion catalyst is a perforated low-density mat made of quartz fibers on which catalytic substances comprising platinum and carriers are impregnated. Fig. 15 is a magnified view of the catalytic fibers.

If the burners fueled by natural gas have the same performance as that fueled by LPG, they may be widely used not only in residential, but also in industrial areas. However, it was reported previously that burners using the same type of catalysts as employed for LPG showed not only a low combustion efficiency, but also a comparatively quick deterioration [1]. In another report, pessimistic perspectives on the development of natural gas fuel-diffusive catalytic burners were published based on the reaction mechanism of methane in the burner [2].

Subsequently, the advent of porous alumina fiber with a large surface area was considered to improve the combustion performance of natural gas drastically, because catalysts manufactured by impregnating the fiber with catalytically active metals can exhibit a greatly increased uniformity and an active-site area as compared with the LPG-catalyst. Fig. 16 is a magnified view of the porous alumina fibers containing 0.5 wt% rhodium.

Trimm et al. [3] performed detailed studies on the kinetics of methane oxidation over a platinum-impregnated porous alumina fiber catalyst and a numerical analysis of the burner with a one-dimensional flow model [4]. However, the authors discussed neither the

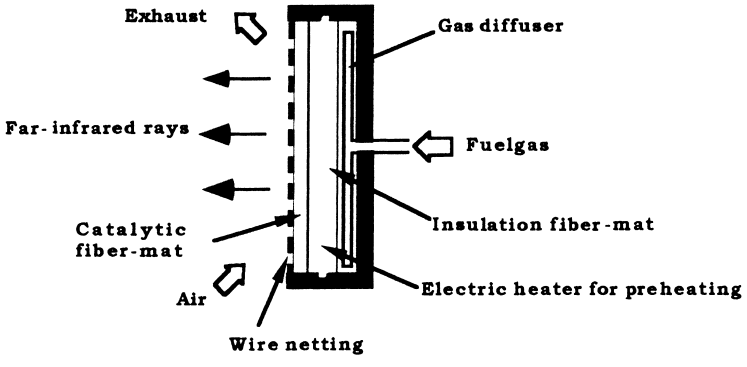

Fig. 1. Basic construction of the diffusive catalytic combustion method.

completeness of methane combustion in the burner nor its reaction mechanism. Kang et al. [5] have recently performed studies on the performance and durability of burners using platinum-group metal-impregnated porous alumina fiber-mats, but such a discussion was not included.

In this section, a detailed experimental analysis of the combustion in a burner fueled by methane using a rhodium-impregnated porous alumina fiber-mat and the oxidation kinetics of methane using a microreactor under the conditions representative for the burner are described with a conceivable mechanism of complete methane combustion.

2.1. *Catalyst for natural gas-diffusive combustion*

It is known that the most active substances for total oxidation of methane are platinum group metals including palladium, rhodium, platinum and the activities of base metal oxides are an order of magnitude lower than that of the least active platinum. Palladium has an outstanding activity, but its activity easily deteriorates at temperatures less than 600°C by even small amounts of sulfur compounds added to natural gas as odorants. The activity of platinum hardly deteriorates by sulfur compounds, but platinum causes erosions of porous alumina fiber-mat, because it has a high activity to convert sulfur compounds to sulfur trioxide, which is easily converted to sulfuric acid in the burner. Rhodium was adopted as a catalytically active substance for methane combustion, because it has intermediate characteristics in activity and susceptibility to sulfur compounds.

The combustion catalyst was manufactured according to the following procedure. An aqueous solution of rhodium chloride was circulated and sprayed over a porous alumina fiber-mat until almost all rhodium chloride in the solution was impregnated. The mat was dried in an oven with circulating hot air and then calcined for 1 h at 600°C in a nitrogen-steam atmosphere. Table 1 shows the rhodium dispersions of the products, whose rhodium contents were from 1 to 0.15 wt%, as measured by the CO pulse adsorption method. It was found that rhodium was dispersed over porous alumina fiber as particles with a diameter of around 1 nm.

Table 1
Rhodium dispersion impregnated over porous alumina fiber-mat

Rh-loading (wt%)	CO-adsorption (N cm^3 g^{-1})	Surface area (m^2 g^{-1})	Particle size (nm)	Dispersion (%)
1.0	1.38	5.08	0.79	63.4
0.55	0.645	2.37	0.93	53.8
0.25	0.376	1.38	0.72	69.0
0.15	0.019	0.07	8.7	57.6

Table 2
Configuration of the test burner

Item	Length (effective) (mm)	Bulk density (kg m^{-3})
Height	170 (150)	–
Width	220 (200)	–
Thickness		
Catalyst-mat	10	38
Insulation-mat A	6	96
Insulation-mat B	12.5	64

2.2. *Combustion measurement of the burner*

Table 2 shows the configuration of the test burner. It was set vertically not to disturb natural convection in a 700 mm×700 mm square box. Catalytic combustion was started using hydrogen gas and then shifted to methane. The purity of methane and hydrogen was 99% and 99.999%, respectively.

The measurement of temperature and composition inside the burner was carried out by inserting a probe integrating a needle-shaped gas sampling tube made of stainless steel whose outer diameter was 0.75 mm with a sheathed chromel–alumel thermocouple whose outer diameter was 0.5 mm, using a traversing device. The sampled gas, maintained at about 70°C not to condense water, was introduced into a gas chromatograph (GC) system by a suction pump. The GC system was capable of analyzing H_2, O_2+Ar, N_2, CH_4, CO, CO_2, C_2H_2, C_2H_4, C_2H_6, C_3H_8, *i*-C_4H_{10}, and *n*-C_4H_{10} simultaneously. The analysis limits of hydrocarbons and CO were 1 ppm, and those of H_2, CO_2 were 10 ppm by mole fraction. The O_2 mole fractions were calculated by the following equation, because O_2 and

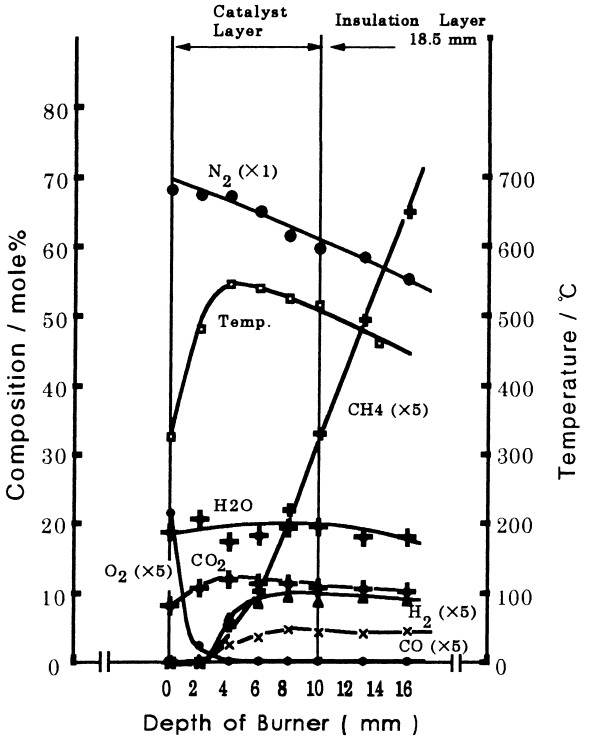

Fig. 2. Gas composition and temperature in the depth of the burner. Fuel: methane>99%; heat load: 17.4 kW m^{-2}.

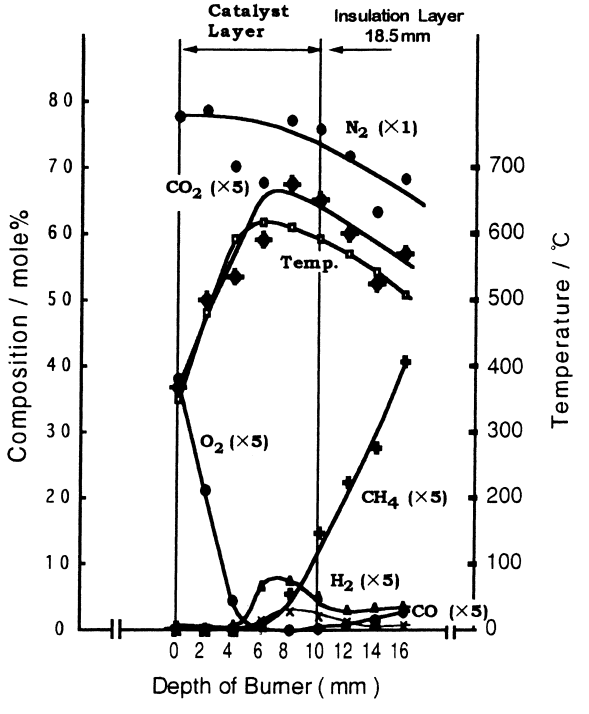

Fig. 3. Gas composition and temperature in the depth of the burner. Fuel: methane>99%; heat load: 11.6 kW m^{-2}.

Ar were not separated:

$$[O_2](\text{calculated}) = [O_2 + Ar](\text{measured}) - 0.0119 \times [N_2](\text{measured}).$$

The brackets [ ] represent the mole fraction and 0.0119 is the Ar/N_2 ratio in air. Water mole fractions were calculated by subtracting the sum of the other components from 100%. The suction speed of gas sampling did not affect the results up to 10 cm^3 min^{-1}, but all measurements were made at 2 cm^3 min^{-1}.

Figs. 2–4 show the results of combustion analysis made by burning methane at heat loads of 17.4, 11.6, and 23.2 kW m^{-2}, respectively, and Fig. 5 shows also the result of burning hydrogen at the heat load of 17.4 kW m^{-2} at the center of the burner. These results show as common features that the oxygen diffused from the front side and the fuel supplied from the back side are mostly consumed and the temperature shows the peak at almost the same position within the catalyst layer. Such features surprisingly look like those of a homogeneous diffusion burner [6]. The mole fractions of methane at the position where oxygen is mostly consumed and at the surface, burning at the heat load of 17.4 kW m^{-2}, were about 600 and about 400 ppm, respectively, and completeness of combustion expressed by the rate of conversion to carbon dioxide was 99.5%. The positions where oxygen and fuel were mostly consumed moved to the surface side with an increase of the heat load. They were 6, 3, and 1 mm from the surface at the heat loads of 11.6, 17.4, and 23.2 kW m^{-2}, respectively. These results clearly show that the combustion performance of the burner is controlled by oxygen diffusion from the front side and the limit of the heat load exists at approximate 23 kW m^{-2}.

In the homogeneous diffusion flame, the features have been elucidated, using a numerical model assuming an infinite reaction rate at the position where the mixture of oxygen and fuel reaches the stoichiometric composition [7]. Accordingly, such a fast reaction model is plausible even in the catalytic burner, but

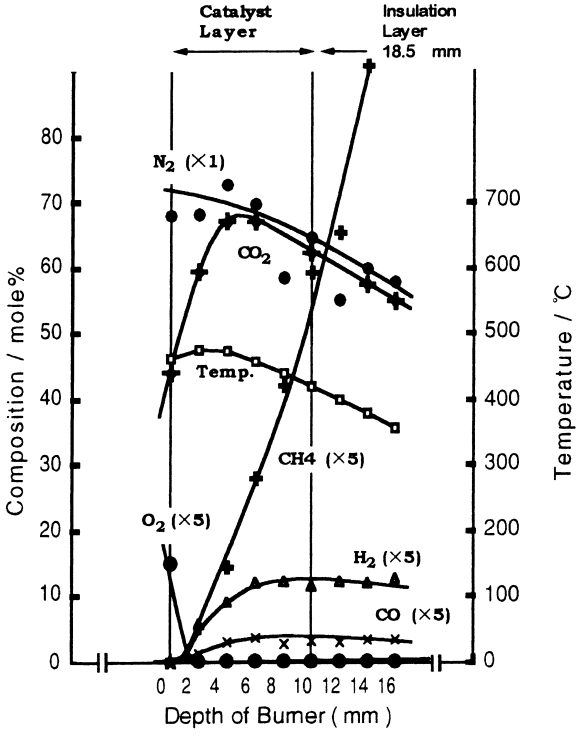

Fig. 4. Gas composition and temperature in the depth of the burner. Fuel: methane>99%; heat load: 23.2 kW m^{-2}.

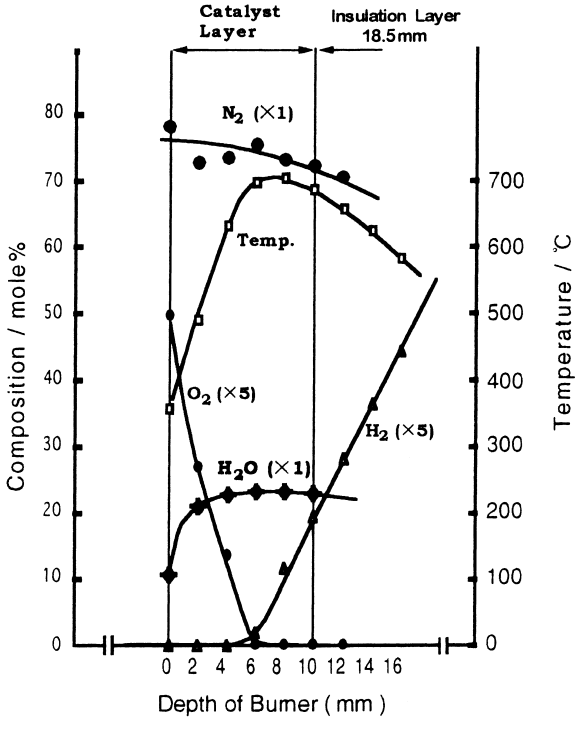

Fig. 5. Gas composition and temperature in the depth of the burner. Fuel: hydrogen>99%, heat load: 17.4 kW/m^2.

the following two problems should be considered. One relates to transfer to pore-diffusion control of the total reaction rate when the reaction rate at the active sites greatly increases. It is quantitatively treated as the effectiveness factor of the catalyst using a one-dimensional Thiele modulus proportional to the catalyst radius [8]. In terms of the fiber catalyst whose mean radius is 0.0015 mm, it is assumed that the effectiveness factor will remain at a high level because the Thiele modulus is so small and that the catalyst has the possibility to maintain a fast surface reaction. The other problem relates to the reactivity of the catalyst. It is difficult to explain such a fast reaction using a total oxidation mechanism. The key to clarifying this problem is the presence of carbon monoxide and hydrogen at the back side of the position where oxygen mostly disappears. Since only carbon monoxide or only hydrogen was analyzed inside the burner in the previous experiments partly because of the analytical device used, the presence of a carbonaceous intermediate-deposition mechanism in the burner was seriously considered [2,3]. Since these experiments always detected both components, the presence of another stable mechanism producing carbon monoxide and hydrogen is plausible. In their paper on methane oxidation over a Ni–alumina catalyst, Wise et al. [9] reported on a very fast partial oxidation producing carbon monoxide and hydrogen after the oxygen overlayer on Ni surface was consumed.

The mole fractions of steam and carbon dioxide in the burner were approximately 20%, and 10%, respectively, which were almost the same as the stoichiometric composition upon complete combustion of methane.

2.3. *Reaction kinetics over Rh–alumina fiber catalyst*

Methane oxidation experiments over Rh–alumina fiber catalysts were carried out to investigate the mechanism of the fast reaction inside the burner using a flow-type microreactor made of a stainless steel tube

whose inner diameter was 15 mm. The catalyst temperature was measured at the top and at 5 mm from the top, using double sheathed-CA thermocouples with a diameter of 0.5 mm. The temperature of the reactor was separately controlled by three block-heaters and the temperature distributions within 100 mm over the catalyst was kept within 1°C under a N_2 gas flow of 100 cm^3 min^{-1}. All the reactant gas-flow rates were controlled by mass flow controllers and water was supplied by a constant-flow pump, then evaporated, and finally mixed with other reactants. The purity of the reactant gas was more than 99.9%, and water was purified by an ion-exchange method. The gas sampled from the outlet gas maintained at about 70°C was introduced into the above GC system by suction and H_2, CO, CO_2, CH_4, CO_2, O_2, and N_2 were analyzed simultaneously.

Almost all the experiments were carried out in the presence of 20% H_2O and 10% CO_2, like the conditions for the burner, and the mole fractions of CH_4 and O_2 were changed, using N_2 as the balance. Methane reaction rates were calculated by the differential method.

Table 3 summarizes the results of total methane oxidation by a 0.73 wt% fresh catalyst, where CO and H_2 were not detected. The apparent reaction orders determined from the results were 1 and 0.5 with respect to CH_4 and O_2, respectively. Since the order of 0.5 with respect to oxygen was the same as that of the Ni–alumina catalyst reported by Wise et al., oxygen seems to react through a dissociatively adsorbed layer on Rh metal according to their discussion.

Table 4 summarizes another result of run 12 (CH_4/O_2=1.0) shown in Table 3, in which the reaction temperature was increased to 506°C and then decreased. Fig. 6 shows the variations of methane conversion. When the methane conversion had increased to about 40%, the conversion suddenly jumped to more than 95% with large amounts of CO, and H_2 with no oxygen in the outlet gas and the high methane conversion with similar outlet gas composition continued at decreasing temperatures down to 400°C. The total carbon mole fraction did not show meaningful variations in this experiment.

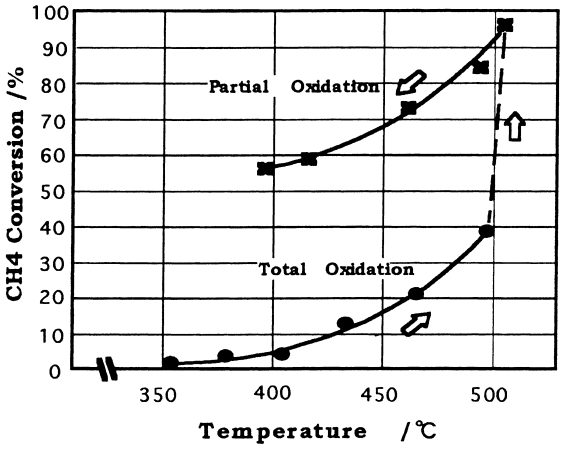

Fig. 6. Hysteresis of methane conversion (run 12 O_2/CH_4=1.0).

Fig. 7 shows the effect of oxygen mole fractions on methane oxidation rates over a sulfur-poisoned Rh–alumina fiber catalyst measured after a 10 672 h combustion life test. The initial rhodium content was 0.55 wt% and the sulfur content after the life test was 0.2 wt%. The methane oxidation rate was proportional to the 0.5th power of the oxygen mole fraction at high oxygen mole fractions but the rate fluctuated irregularly at higher levels at lower oxygen mole

Table 3
Methane total oxidation over Rh–fiber-mat catalyst under excess of steam and carbon dioxide

Run no.	X_{CH_4}	X_{O_2}	T_4 (°C)	Conversion (%)	AE (kcal mol^{-1})	r at 400°C (mol kg^{-1} min^{-1})
13	0.0222	0.0888	378–479	~56	21.2	0.115
10	0.0046	0.0904	377–506	~72	15.8	0.031
8	0.0090	0.0900	377–459	~49	20.1	0.060
18	0.0090	0.0900	378–433	~38	22.7	0.066
12	0.0238	0.0238	352–492	~38	21.1	0.060
11	0.0232	0.0465	377–463	~27	21.1	0.066

X: mole fraction; T_4: temperature at 5 mm from the top of the catalyst; Conversion: methane conversion; AE: activation energy; r: methane reaction rate at 400°C.

Table 4
All data of run 12 (O_2/CH_4=1.0)

T_4 (°C)	T_3 (°C)	CH_4 (%)	O_2 (%)	CO (%)	H_2 (%)	CO_2 (%)	TC (%)	Conversion (%)	r (mol kg^{-1} min^{-1})
352	352	2.36	2.51	ND	ND	9.67	12.03	1.7	0.017
378	377	2.25	2.35	ND	ND	9.47	11.72	3.9	0.040
404	403	2.26	2.30	ND	ND	9.57	11.80	4.6	0.047
432	430	2.04	1.95	ND	ND	9.75	11.89	13.5	0.140
464	460	1.95	1.54	ND	ND	10.3	12.25	20.8	0.215
497	492	1.42	0.60	ND	ND	10.2	11.62	38.7	0.402
506	500	0.106	N.D.	0.593	1.70	10.7	11.40	95.4	0.991
484	476	0.403	N.D.	0.500	1.48	11.6	12.50	83.9	0.872
461	452	0.646	N.D.	0.291	0.951	12.0	12.94	73.1	0.759
416	405	0.990	N.D.	0.090	0.395	11.0	12.08	59.2	0.615
396	383	1.05	N.D.	0.047	0.286	10.8	11.90	55.9	0.581

T_4: temperature at 5 mm from the top of the catalyst; T_3: temperature at the top of the catalyst; TC: total carbon mole percent; Conversion: methane conversion; r: reaction rate of methane at 400°C.

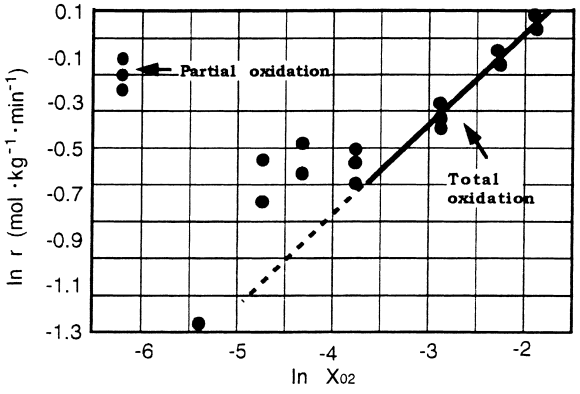

Fig. 7. Effect of oxygen mole fractions on methane reaction rates over a sulfur-poisoned catalyst. Temperature: 528°C; mole fraction of reactants: CH_4=0.025; H_2O=0.20; CO_2=0.10; O_2=Xo_2.

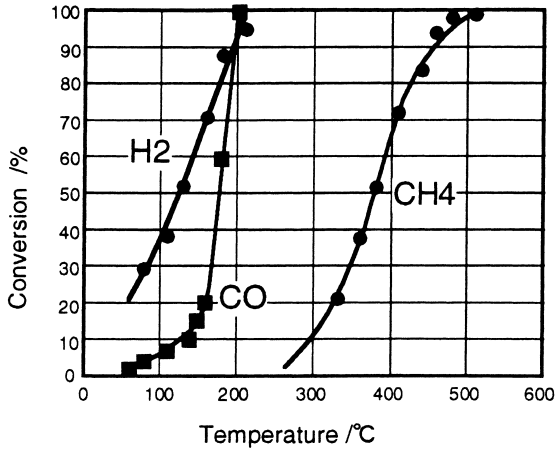

Fig. 8. Reactivity of methane, hydrogen, carbon monoxide over rhodium alumina fiber catalyst. Catalyst: 100 mg; flow rate of reaction: fuel gas=0.5 cm^3 min^{-1}; O_2=10.0 cm^3 min^{-1}; N_2=39.5 cm^3 min^{-1}.

fractions, viz less than 0.05, and finally stabilized at a high level with H_2, and CO with no O_2 in the outlet gas.

Fig. 8 shows the reactivity of CO, H_2, and CH_4 over a fresh Rh–alumina fiber catalyst under an excess of O_2. The reactivity of H_2 and CO was so high that they were completely converted when CH_4 started reacting.

Mild steam reforming reactions in the experiments without oxygen over the fresh catalyst were observed; but not over the catalyst poisoned by sulfur compounds. The possibility of other side reactions producing carbonaceous intermediates was considered, but the contribution of those reactions was assumed to be small because partial oxidation was stable and the carbon-balance of the reaction streams was good.

In conclusion, it was found that at least two stable mechanisms exist in oxidation of methane under excess H_2O and CO_2 over Rh–alumina fiber catalysts. One is mild total oxidation and the other is partial oxidation at very high conversion levels producing H_2 and CO. H_2 and CO exhibit a very high reactivity under excess O_2 as compared with that of methane. Accordingly, total oxidation of methane at an apparent very high rate in the diffusive catalytic burner is

assumed to proceed via partial oxidation of methane and consecutive oxidation of H_2 and CO.

In terms of this mechanism, completeness of methane combustion under conditions that the gas flow in the burner still contains oxygen may not be attained, since only mild total oxidation occurs. This agrees with the results of the simulation by Trimm et al. [4], who assumed a total oxidation mechanism, while numerical analysis adopting an infinite reaction model well explained the combustion features of the burner described above [10].

2.4. *Applicability of diffusive catalytic combustors fueled by natural gas*

The author investigated application of diffusive catalytic combustors fueled by natural gas, using Rh–alumina fiber-mat catalysts in residential and industrial uses and finally commercialized modular burners for general use, commercial radiant heaters, industrial textile dryers, industrial adhesive process heaters, etc.

The diffusive catalytic combustors fueled by natural gas have prominent merits; such as nearly no-NO_x, high far-infrared radiation efficiency, fire safety, and temperature uniformity, but have drawbacks such as time-consuming start-up, need for proper control of secondary air supply to attain high combustion efficiency, and high catalyst cost.

Further improvements on the catalyst and application device are expected in order to extend the above applications.

3. Adiabatic lean premixed catalytic combustion

Although many application studies of this concept to gas turbine combustors have been carried out since having been proposed by Pfefferle et al. [11] in the early 1970s, its commercialization has been hindered by the difficulty of producing high-temperature-durable combustion catalysts. Transition-metal-substituted hexaaluminate catalysts, which were developed by Arai et al. [12] in the mid-1980s, have been expected to overcome this technical barrier, because they have prominent characteristics, such as having almost the same threshold temperature of combustion as platinum catalysts, much higher durability, and formability as an active monolith.

The author was engaged in the development of ceramic combustion catalysts directly formed in honeycomb shape from the transition-metal-substituted hexaaluminate powder and their application to cogeneration gas turbine combustors from 1988 to 1995 [13,14]. The targets were 1500 kW class gas turbines with 9 atm, abs. standard operating pressure, 1100°C maximum operating temperature, and 40 ppm (converted at O_2 0%) of NO_x emissions, which are of the same order of magnitude as that of gas engine cogeneration systems adopting NO_x reduction systems for the exhaust using a three-way catalyst. The above targets were thought to be hardly attainable by homogeneous lean premixed combustion methods.

Fig. 9 shows the catalytic combustor concept which was developed by Kawasaki Heavy Industries [15]. A homogeneous diffusive type precombustion burner is used for the turbine start-up and for keeping the catalyst inlet temperature in steady state. An air bypass valve at the outlet of the catalyst is used for quick response and proper control of the catalytic combustion corresponding to variations in the turbine load. The operating temperature of catalytic combustion at the rated turbine load was set at 1200°C. The target durability was more than 8000 h and 400 on–off cycles.

3.1. *Development of a ceramic combustion catalyst*

Although optimum compositions of the transition-metal-substituted hexaaluminate catalyst were investigated regarding activity and durability; in the manufacturing process, $Sr_{0.8}La_{0.2}MnAl_{11}O_{19-\alpha}$ which was proposed by Arai et al. [12], was the best one. The powder was manufactured via the sol–gel method using an alkoxide solution of strontium and aluminum and an aqueous solution of manganese and lantanum salts, although precipitation from aqueous solutions containing all the metal salts was also possible. Fig. 10 shows the relationship of methane oxidation activity, specific surface area, bending strength, and calcination temperature of the ceramic honeycomb catalysts. From these results, the maximum calcination temperature was determined to be 1300°C. The two kinds of ceramic catalysts shown in Table 5 were manufactured. Since the thermal shock resistance of

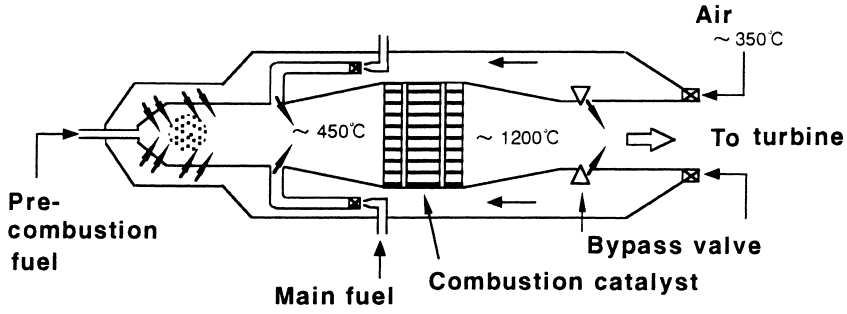

Fig. 9. Schematic construction of the catalytic combustor for gas turbine.

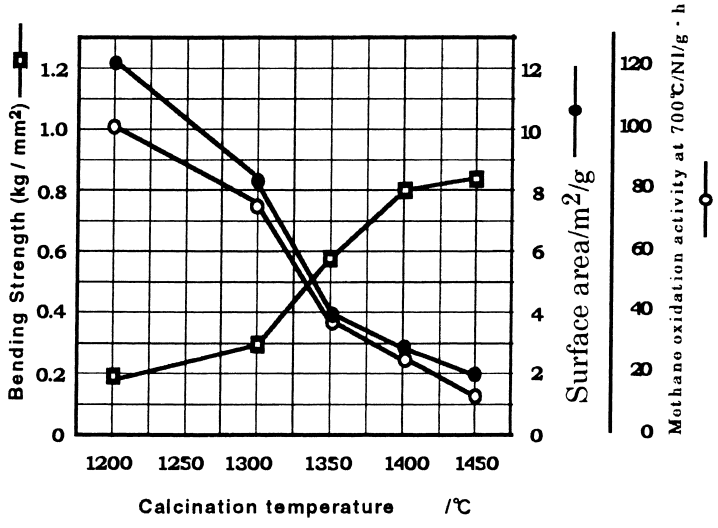

Fig. 10. Relationship between strength, surface area, and activity with calcination temperature of the ceramic honeycomb catalyst.

Table 5
Properties of the ceramic combustion catalyst

Properties	1200°C-calcined catalyst	1300°C-calcined catalyst
Structural properties		
Cell pitch (mm)	1.57	1.53
Wall thickness (mm)	0.30	0.29
Cell height (mm)	20	20
Mechanical properties		
Bulk density (kg m^{-3})	630	670
Bending strength (MPa)	13.3	28.0
Young modulus (GPa)	8.75	16.0
Coefficient thermal strength ($°C^{-1}$)	8.8×10^{-6}	8.8×10^{-6}

the catalysts was fairly low, i.e. approximately 400°C, the catalyst holder shown in Fig. 11 was developed for scaling-up. Within the catalyst holder segmented catalysts are loosely packed both in the axial and radial directions. The configuration of the segmented catalysts in the radial direction was designed by thermal stress simulation modeled by the finite element method using two-dimensional beam elements [16].

3.2. A multiple catalyst system and its performance

The threshold temperature of combustion of the ceramic catalysts is thus high that a multiple catalyst system using platinum group metal-supported honeycomb catalysts is inevitable to attain the NO_x emis-

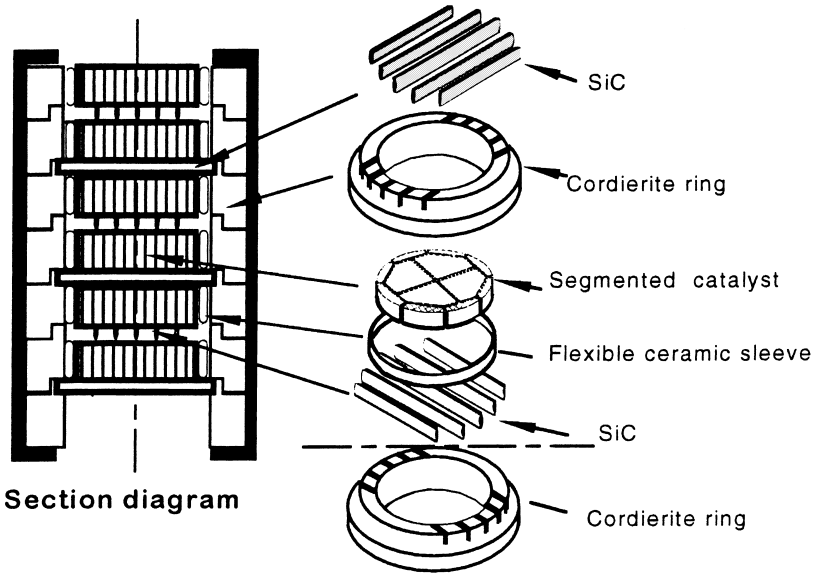

Fig. 11. Schematic construction of the catalyst holder.

sion-targets with application to gas turbine combustors. Palladium is the most efficient catalytically active material for the front-stage catalyst, since it has superior activity for total methane oxidation and sulfur poisoning as described above will be avoidable because the surface temperature will be over 600°C.

A practical palladium catalyst for the front-stage was prepared by wash-coating a slurry containing palladium powder with a mean diameter of 1 μm, promoters, and stabilized alumina support into a 200 cpi cordierite honeycomb.

Fig. 12 shows the wall and gas-phase temperatures inside a catalyst system of a diameter of 50 mm consisting of one layer of palladium catalyst, four layers of ceramic catalysts calcined at 1200°C, and two layers of ceramic catalysts calcined at 1300°C mounted consecutively from the front, burning natural gas (CH_4 88%, C_2H_6 6%, C_3H_8 4%, C_4H_{10} 2%, sulfur

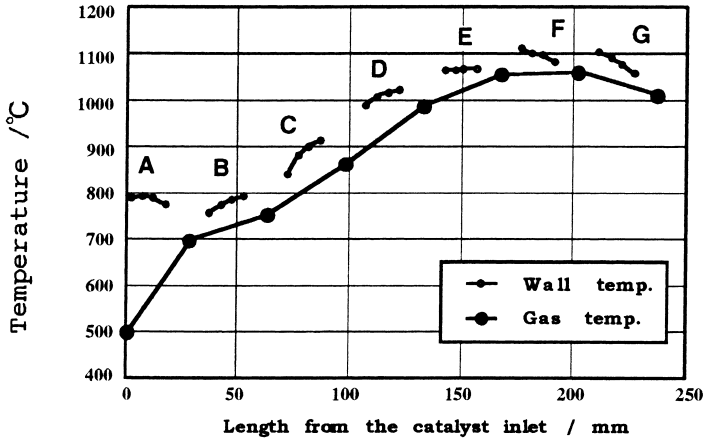

Fig. 12. Combustion features of natural gas with the high-temperature catalyst system at atmospheric pressure. A: palladium catalyst; B, C, D, E: 1200°C-ceramic catalyst; F, G: 1300°C-ceramic catalyst; pressure: 1 atm; catalyst inlet temperature; 500°C; theoretical adiabatic temperature: 1200°C; catalyst inlet linear velocity: 3.5 ms^{-1} (at 0°C).

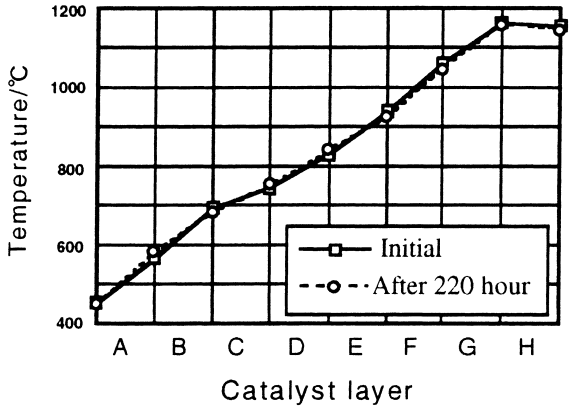

Fig. 13. Axial gas temperature profiles of the catalyst layer at the beginning and the end of 220 h combustion test at 1 MPa.

compounds 5 ppm) at atmospheric pressure. The fuel–air mixture was preheated by indirect gas and electric heaters. The catalyst part was sufficiently insulated. The temperatures were measured by 1 mm diameter chromel–alumel thermocouples mounted approximately at the center. The thermocouples for measuring wall temperatures were inbeded in one cell whose inlet was closed by ceramic adhesive. The wall temperatures of the layer containing the palladium catalyst were almost 800°C along the entire length of the cell and did not show any oscillation. It was well in accordance with the dissociation temperature of PdO as referred to in many references [17], while the wall temperatures of the ceramic catalysts showed a trend to increase with the wall length up to 1000°C as in surface reaction control. Accordingly, the system could not attain satisfactory combustion performance even at higher velocities under the conditions where the operating temperature was adjusted to less than 1200°C.

Fig. 13 shows the axial gas temperature profile of a 50 mm diameter catalyst system at the beginning and the end of a 220 h natural gas combustion test at 1.0 MPa. The system consisted of two layers of palladium catalyst, three layers of ceramic catalysts calcined at 1200°C, and three layers of ceramic catalysts calcined at 1300°C. The fuel–air mixture was preheated by an electric heater. The catalyst part was insulated by a ceramic fiber mold of a thickness of 20 mm. The hot exhaust gas from the catalyst was cooled by air at a point 140 mm behind the catalyst. Gas analysis was carried out at the outlet of the device. Both axial gas temperatures show almost the same profile with a smooth increase and it appeared that combustion had nearly completed in the catalyst, since the outlet temperature of the seventh layer approximately reached the theoretical adiabatic temperature of the inlet mixture. The total oxidation extent of natural gas calculated from gas analysis was more than 99.9% and NO_x production was scarcely detected. Since changes in specific surface area of the catalysts before and after 220 h continuous operation were so small; it can be concluded that the catalyst could exhibit a satisfactory durability even in high-pressure operation. Table 6 shows the operating range of the system with respect to linear velocity at the catalyst inlet, inlet temperature, and theoretical adiabatic temperature.

3.3. *Evaluation of a high-temperature catalytic combustion system in a 160 kW gas turbine-test device*

A prototype catalytic combustor for gas turbines equipped with a segmented catalyst system 220 mm in diameter, schematically shown in Fig. 9, was prepared and tested in a 160 kW gas turbine test device. The ceramic catalysts were segmented into 12 portions. The nominal turbine pressure ratio, air flow rate, and combustor inlet air temperature under standard conditions were 8.5, 1.8 kg s^{-1}, and 350°C, respectively.

Table 6
Operating range of the high-temperature catalyst system

Pressure (MPa)	Catalyst inlet temperature (°C)	Catalyst outlet temperature (°C)	Catalyst inlet linear velocity[a] (m s^{-1})
1.0	450–500	1200	2.6–3.0
1.0	450–500	1150	2.2–2.6
1.0	450–500	1100	1.9–2.2

[a]At 0°C.

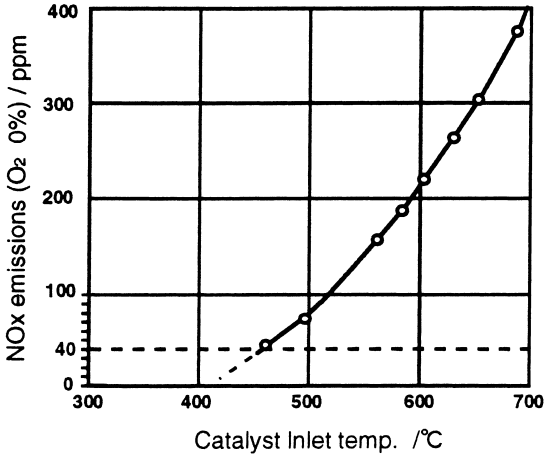

Fig. 14. Relationship between the catalyst inlet temperature and NO_x emissions by the turbine test device.

The turbine load was adjusted by an eddy-current dynamometer. The operations related to the catalyst inlet temperature, the turbine load, the air bypass valve, and the turbine speed were manually controlled, while the total fuel flow rate was automatically controlled according to the turbine speed. Natural gas, whose composition was given above, was used as fuel. The details are omitted here since they have been described in other references [13,14].

As a result, the catalyst system was demonstrated to attain the target performance and to have long-term durability because it did neither show performance changes during a 215 h continuous operation test at the rated load, nor crack generation in repeated sudden stop tests in which the catalytic combustor turbine at the rated load was suddenly stopped five times in total after at least a half hour steady-state operation.

Fig. 14 shows the relationship between NO_x emissions and mean catalyst inlet temperatures obtained by this test device in which a precombustion burner with a conventional homogeneous diffusion burner was used. It is assumed that NO_x was produced in the precombustion burner because it was scarcely produced in the tests at 1.0 MPa without a precombustion burner, such as the one described above. The mean catalyst inlet temperature is required to be lowered at least to 450°C to attain the 40 ppm NO_x emissions target surely as long as the precombustion burner has not been improved on NO_x reduction.

Fig. 15 shows the basic control concept for the commercial catalytic combustor turbine which has been developed by Kawaski Heavy Industries [15]. Applicability of the concept was confirmed by another test measuring the response of the turbine speed and the catalyst outlet temperature to a stepwise change of the fuel control valve and the air bypass valve, respectively, at different turbine loads.

In conclusion, applicability of the high-temperature catalytic combustion system to a 1.5 MW turbine combustor has been demonstrated through prototype catalytic turbine tests.

However, in very recent years, non-catalytic homogeneous lean premixed combustors for gas turbines fueled by natural gas have noticeably been improved [18]. The 1.5 MW compact combustor without air bypass valves which realizes 75 ppm of NO_x emissions in a 75–100% load range has been commercialized [19]. Also, 250 kW prototype gas turbine tests with an air bypass valve have demonstrated 35 ppm of NO_x emissions in a 90–100% load range [20]. The concept of these combustors is based on attaining totally lean combustion by introducing a lean fuel–air mixture at the periphery or the back side of a diffusion-flame burner with multiple nozzles.

The principal drawback of the high-temperature catalyst system based on Mn-substituted hexaaluminate monolithic honeycomb catalysts fueled by natural gas is that the throughput is so low that installing it on a conventional engine package may not be possible.

Commercialization of the system has therefore been suspended in these situations.

3.4. *Future directions for adiabatic lean premixed catalytic combustion*

Although improvements of the homogeneous lean premixed combustion method have been remarkable, it has intrinsic problems derived from its lean combustion limit, such as combustion fluctuations easily occurring at variations of the turbine load and also low NO_x emissions hardly being maintained particularly at low turbine loads where fuel becomes totally lean.

Accordingly, the catalytic combustion method is still expected to be effective in the solution of such problems. Since the use of compact combustors is inevitable, the hybrid catalytic combustion concept

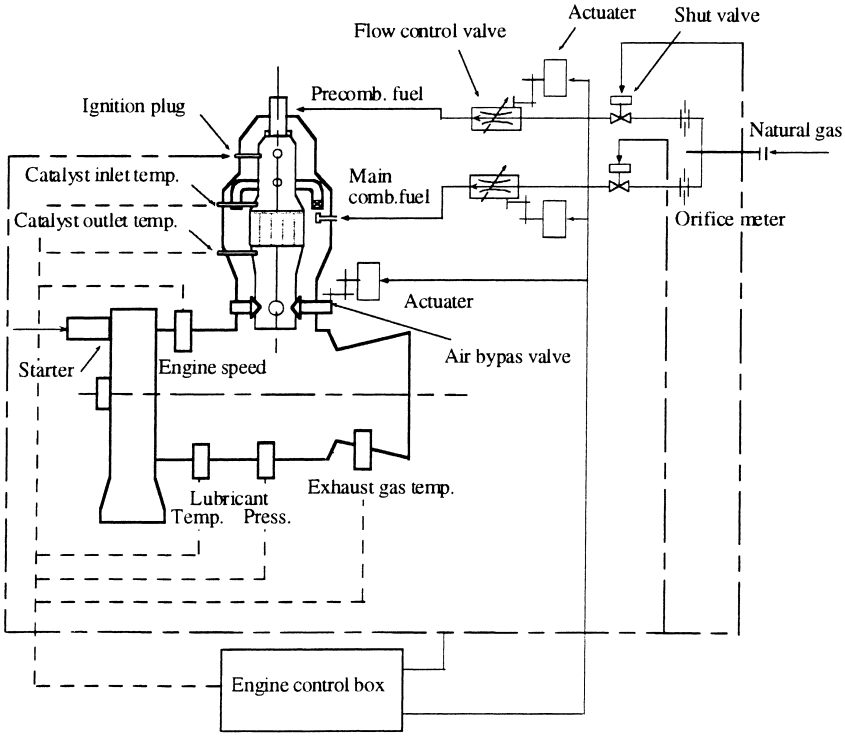

Fig. 15. Basic controls for catalytic combustor turbine.

consisting of a low-temperature catalytic combustion zone and a gas-phase combustion zone downstream the catalyst may be better in future, because it will probably attain much higher throughputs than that of the high temperature-catalytic combustion concept.

Two types of concepts have been proposed for the hybrid system. One adds secondary fuel to induce gas-phase oxidation downstream the catalyst [21,22]. The other supplies all the fuel to the catalyst while controlling reactions to maintain the catalyst temperature below the durability limit [23]. The latter concept may be better for small-scale combustors, of which simplicity is required, although the development of the catalyst is more difficult than that of the former concept. The catalyst is expected to be operative at an inlet temperature of about 350°C with hardly any need of a precombustion burner in steady-state operation and to yield as high outlet temperatures as possible up to 1000°C to propagate gas-phase oxidation easily at high linear velocities.

The hybrid catalytic combustion system with such catalysts may enable new residential and industrial applications other than gas turbine combustors, e.g. unvented residential heaters and industrial dryers for drying processes in which nearly zero NO_x emissions are required.

4. Radiant premixed catalytic combustion method

Application studies of this concept using platinum group metal-supported cordierite honeycomb catalysts have been carried out to reduce NO_x emissions from unvented residential heaters fueled by liquid fuel widely used in Japan for many years. Also, evaluation of the application of unvented residential heaters fueled by natural gas has already been carried out. The work demonstrated NO_x emissions less than 5 ppm (at O_2 0%) with a prototype heater, but the heater was not commercialized because the turndown rate was a little low and the cost was high.

As industrial uses, applications to a water-tube boiler with combustion taking place among cata-

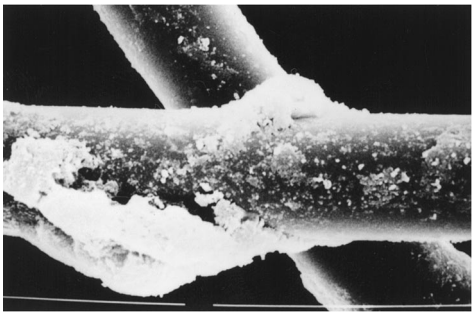

Fig. 16. Magnified view of catalytic fibers for LPG-combustion.

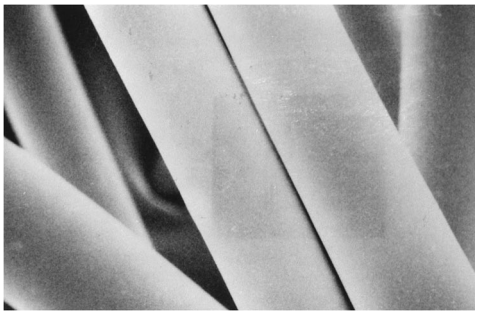

Fig. 17. Magnified view of catalytic fibers for natural gas combustion.

lyst-coated water tubes [24], a radiant furnace with combustion in small tubes with catalyst-coated inner surface [25], a planar radiant burner using a cloth-shaped catalyst at the surface, a water boiler using a catalyst fluidized bed, and a paint dryer using a fiber-mat catalyst [26] have been investigated. However, those studies, in view of commercialization, have not been satisfactory because there were problems of catalyst deterioration in high-temperature operations and problems of low throughput in low-temperature operations.

In conclusion, future progress of this concept of combustion fueled by natural gas would be limited unless a drastically efficient catalyst is developed.

References

[1] S.W. Radcliffe, C. Migase, J. Inst. Fuel, (1975) 208.
[2] M.R Dongworth, A. Melvin, Proceedings of the 16th International Symposium on Combustion, 1976, p. 255.
[3] D.L. Trimm, C. Wailam, Chem. Eng. Sci. 35 (1980) 1405.
[4] D.L. Trimm, C. Wailam, Chem. Eng. Sci. 35 (1980) 1731.
[5] S.K. Kang, S.M. Moon, I.S. You, Y.O. Ha, Proceedings of the Second International Workshop on Catalytic Combustion, 1994, p. 10.
[6] H.C. Hottel, W.R. Hawthorne, Proceedings of the Third International Symposium on Combustion, 1949, p. 254.
[7] S.P. Burke, T.E.W. Schumann, Ind. Eng. Chem. 20 (1928) 998.
[8] E.W. Thiele, Ind. Eng. Chem. 31(7) (1939) 916.
[9] H. Wise, M. Quinlan, PB 86-214012 (1986).
[10] C.M. Ablow, H. Sadamori, Comb. Sci. Tech. 55 (1987) 1.
[11] L.D. Pfefferle, W.C. Pfefferle, Catal. Rev.-Sci. Eng. 29(2)(3) (1987) 767.
[12] M. Machida, K. Eguchi, H. Arai, Chem. Lett. (1987) 767.
[13] H. Sadamori, T. Tanioka, T. Matsuhisa, Catal. Today 26 (1995) 247.
[14] H. Sadamori T. Tanioka T. Matsuhisa, Proceedings of the 1995 Yokohama International Gas Turbine Congress, vol. 1, 1995, p. 247.
[15] S. Kajita, Y. Tanaka, J. Kitajima, ASME 90-GT-89, 1990.
[16] A. Furuya, T. Nishida, T. Matsuhisa, Proceedings of the Second International Workshop on Catalytic Combustion, 1994, p. 70.
[17] R.J. Farrato, J.K. Lampert, M.C. Hobson, E.M. Waterman, Appl. Catal. B 6 (1995) 263.
[18] L.B. Davis, Proceedings of the 1995 Yokohama International Gas Turbine Congress, vol. 1, 1995, p. 237.
[19] S. Kajita, Fuel and Comb. (Japan) 62(12) (1995) 883.
[20] S. Hayashi, H. Yamada K. Shimodaira, Proceedings of the 1995 Yokohama International Gas Turbine Congress, vol.1, 1995, p. 261.
[21] T. Furuya, K. Sasaki, Y. Hayakawa, K. Mituyasu, Proceedings of the Second International Workshop on Catalytic Combustion, 1994, p. 162.
[22] Y. Ozawa, T. Fujii, S. Kikumoto, M. Sato, H. Fukuzawa, Proceedings of the Second International Workshop on Catalytic Combustion, 1994, p. 166.
[23] R.A. Dalla Betta, J.C. Schlatter, M. Chow, D.K. Yee, T. Shoji, Proceedings of the Second International Workshop on Catalytic Combustion, 1994, p. 154.
[24] J.P. Kesselring, W.V. Krill, S.J. Anderson, M.J. Friedaman, PB-81-236150 (1981) 181.
[25] J. Lannutti, R. Schreiber, PB 86-201639 (1986).
[26] L. Blanchard, M.C. Marion, E. Garbowski, M. Primet, Eurogas 90 (1990) 345.